- Technical Paper -

INITIAL DAMAGE OBSERVATIONS FROM AN E-DEFENSE SHAKE TABLE TEST OF A BUILDING WITH POST-DISASTER FUNCTIONS

Trevor Z. YEOW [*1], Koichi KUSUNOKI [*2], Izumi NAKAMURA[*3], and Yo HIBINO[*4]

ABSTRACT

Shake-table tests of a 3-story reinforced concrete building with post-disaster functions were performed at E-Defense. In the specimen, cladding wall elements were casted to be monolithic with the frame elements with seismic slits present at intended regions of plasticity. Slits at the roof-level and at the column base were filled with concrete to allow these walls to act in compression. It was found that the gap detailing helped the specimen achieve more stringent performance objectives required for buildings with post-disaster functions.

Keywords: E-Defense, shake-table test, post-disaster functions, damage evaluation, crack observations

1. INTRODUCTION

To ensure post-earthquake functionality of buildings of importance, the structural design criteria for these buildings was made more stringent; where (i) the design base shear coefficient must be at least 0.55, and (ii) elements must remain elastic and the maximum permitted interstory drift should not exceed 0.33% at the Japanese Building Code design-level shaking [1].

A detailing was proposed where concrete spandrel wall elements were casted to be monolithic with frame elements, with seismic slits present at intended regions of plasticity to avoid wall reinforcing buckling failure. Static loading tests of such detailing exists [2,3], but no dynamic tests had been conducted. Furthermore, new modifications were proposed to fill the slits with concrete to allow the walls to act in compression.

As part of the Tokyo Metropolitan Resilience Project Subgroup C [4], one-directional shake-table tests of a reinforced concrete building with post-disaster functions were performed at E-Defense. This paper will provide a description of the overall test program, summarize preliminary test observations and damage evaluation outcomes, and assess if the building's design objectives were satisfied.

2. TEST DETAILS

2.1 Structural details

The reinforced concrete building (80% scaled) is shown in Fig. 1. The building was 3-stories tall, 2-bays wide in the direction parallel to the applied shaking, and 1-bay wide in the perpendicular direction. Further structural details had been previously published [5].

Cladding wall elements were casted to be monolithic with frame elements parallel to the shaking-direction, as shown in Fig. 2. Slits with 50 mm width were present at the ends of horizontal walls on 2F and 3F (Fig. 2a), while the slits at RF and column bases was filled with concrete (Fig. 2b).

2.2 Instrumentation

A wide range of instrumentation was installed, such as accelerometers (Fig. 3a), laser transducers (Fig. 3b) and potentiometers (Fig. 3c). Others included strain gauges, 3D scanning equipment, video cameras and optical sensors; amongst others.

2.3 Input excitations

The specimen was subjected to an artificial record five times. The unscaled record was representative of the Japanese Building Code design spectra. The acceleration history and 5% damped response spectra are shown in Fig. 4, and scale factors adopted were:

(i) 0.2 (for serviceability check);
(ii) 1.0 (for checking if interstory drifts were less than 0.33% and that behavior was mostly elastic at Japanese Building Code design-level shaking);
(iii) 1.5 run 1 (representative of design demands for buildings with post-disaster functions);
(iv) 1.5 run 2 (to check if building can survive an aftershock with same intensity as design demand);
(v) 1.6 (to observe building's capability of withstanding multiple strong excitations).

White noise was applied before/after each test to track changes in the building's dynamic properties. These results were not discussed in this paper.

*1 Project Researcher, Earthquake Research Institute, University of Tokyo, JCI Member
*2 Professor, Earthquake Research Institute, University of Tokyo, JCI Member
*3 Chief Researcher, National Research Institute for Earth Science and Disaster Resilience
*4 Associate Professor, Graduate School of Environmental Studies, Nagoya University, JCI Member

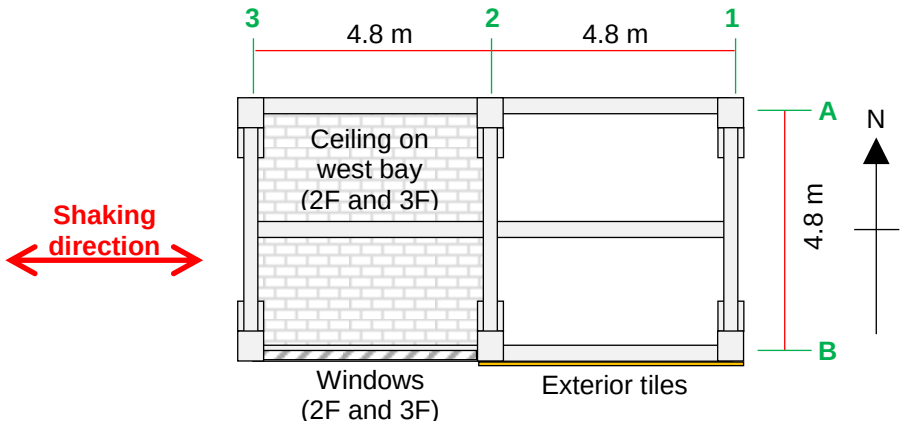

(a)

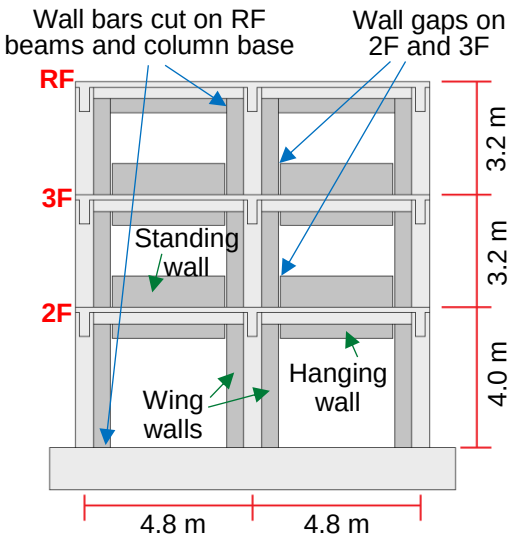

(b) (c)

Fig.1 Specimen structural layout; (a) plan view, (b) in-plane elevation dimensions, and (c) photo

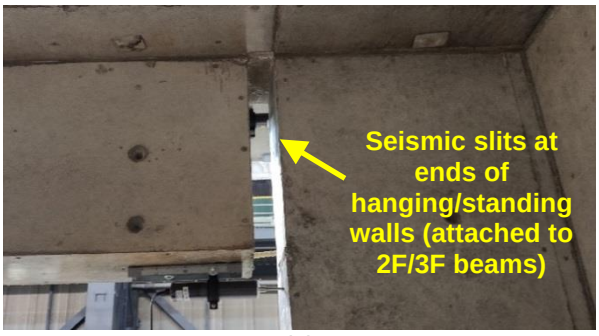

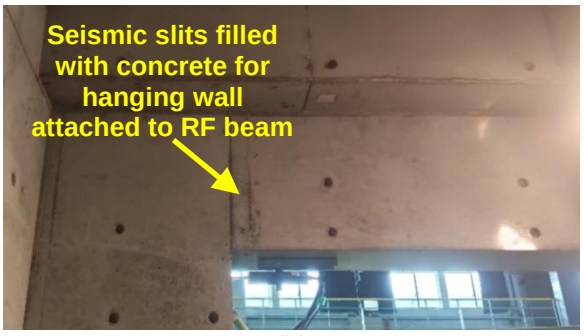

(a) (b)

Fig.2 Detailing at hanging/standing walls ends, (a) 50 mm gap at ends of hanging/standing walls attached to 2F/3F beams, and (b) concrete filled gap on roof level beams (wall longitudinal reinforcing terminated)

(a) (b) (c)

Fig.3 Building instrumentation; (a) accelerometers, (b) laser transducers, and (c) potentiometers

3. PRELIMINARY DAMAGE OBSERVATION

Propagation of cracks for the B1 beam-wing wall joint on 2F and 3F, the base of the A2 column on 1F, and the 3F floor slab are shown in Fig. 5; where B1 and A2 are coordinates following Fig. 1a and the location of new cracks observed after the 1.0-scaled, 1.5-scaled (first run), and 1.6-scaled events were color-coded. Damage photos for these four elements are shown in Figs. 6-9, respectively.

Generally, larger cracks were observed at the B1 beam-wing wall joint at 3F compared to that located at 2F. However, this large crack formed in the hanging wall where there was no reinforcing. In the beam element itself, the residual crack widths were smaller on 3F compared to 2F. Furthermore, concrete spalling was minor on 3F.

For the A2 column, most damage concentrated at the corners of the wing wall. This was expected since these portions would be subjected to high compressive strains. While some horizontal and diagonal cracks did occur in the column, the residual crack widths were generally less than 1.0 mm even after the 1.6-scaled event.

Thin cracks formed after the 1.0-scaled event on the 3F slab and originated near horizontal wall slits. The cracks eventually propagated the length of the slab, and had large residual crack widths over 10 mm after the 1.6-scaled event. Furthermore, 45° diagonal cracks started forming from the columns towards the central beam underneath the floor slab, indicating a secondary mode of force transfer due to the large cracks hindering the predominant force transfer mode.

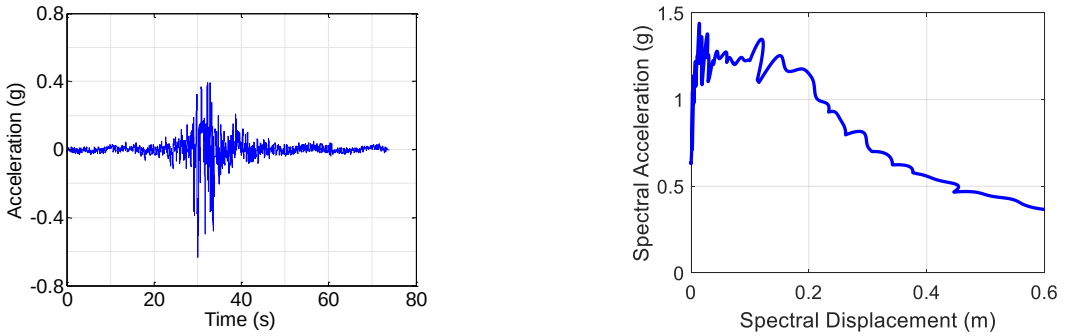

(a) (b)

Fig.4 Artificial record with 1.0 scale factor; (a) total acceleration history, (b) 5% damped response spectra

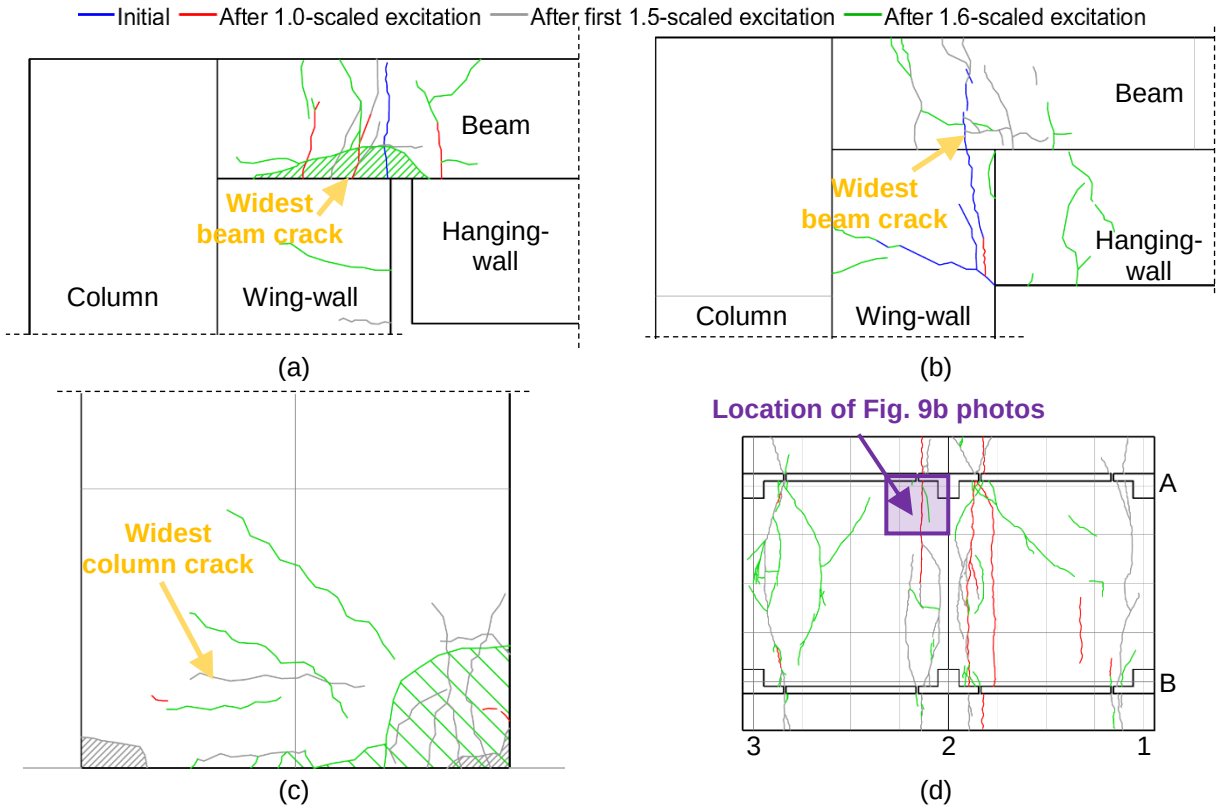

(a) (b) (c) (d)

Fig.5 Crack patterns in various structural members; (a) 2F-B1 beam-wing wall joint, (b) 3F-B1 beam-wing wall joint, (c) 1F-A2 column base, and (d) 3F floor slab

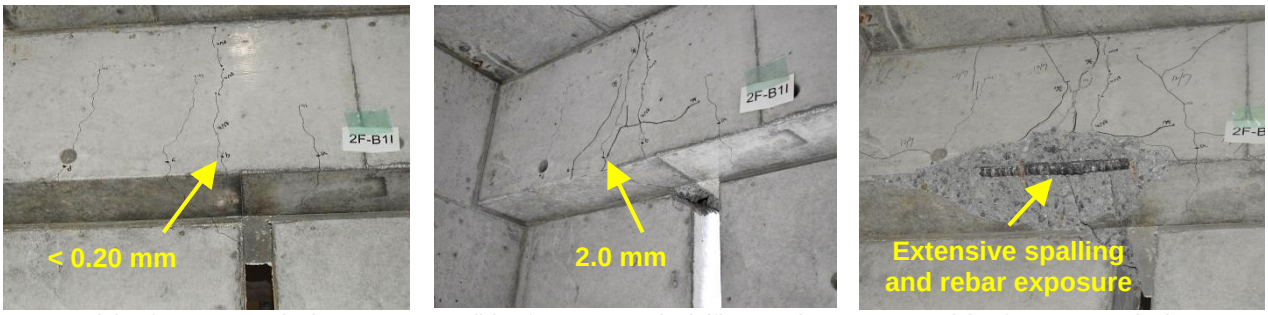

(a) After 1.0-scaled (b) After 1.5-scaled (first run) (c) After 1.6-scaled

Fig.6 Progression of damage in 2F-B1 beam-wing wall joint (residual widths of largest crack indicated)

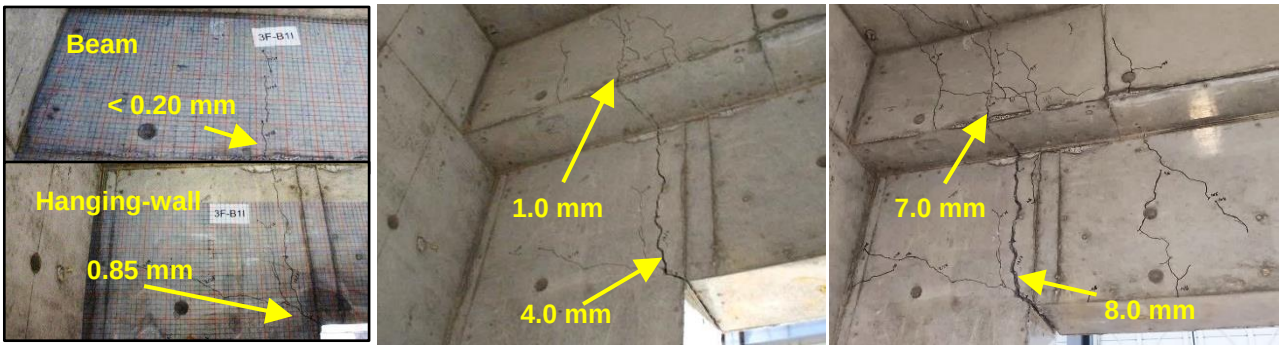

(a) After 1.0-scaled (b) After 1.5-scaled (first run) (c) After 1.6-scaled

Fig.7 Progression of damage in 3F-B1 beam-wing wall joint (residual widths of largest crack indicated)

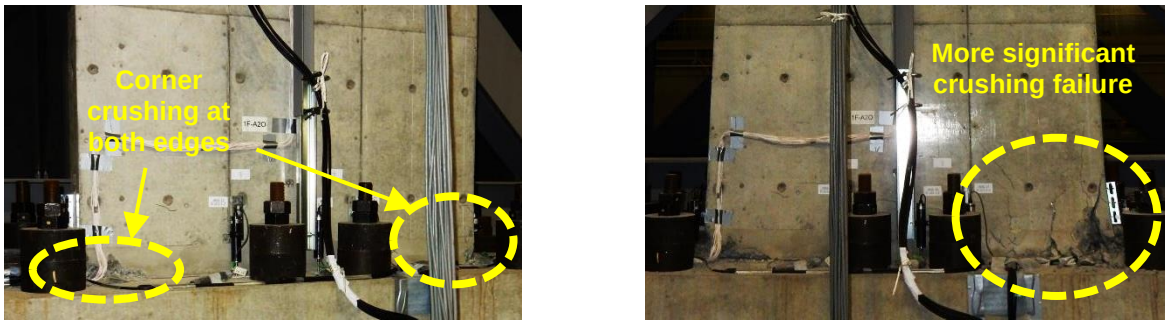

(a) After 1.5-scaled (first run) (b) After 1.6-scaled

Fig.8 Progression of damage in 1F-A2 column base (insignificant damage observed after 1.0 scaled input and thus photo not included; significant damage indicated)

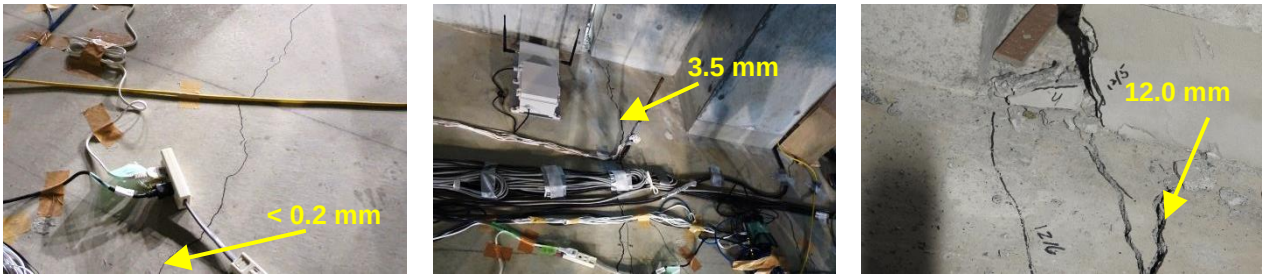

(a) After 1.0-scaled (b) After 1.5-scaled (first run) (c) After 1.6-scaled

Fig.9 Progression of damage in 3F floor slab (residual widths of largest crack indicated)

4. DAMAGE EVALUATION

4.1 Visual damage inspection

Damage evaluation of the building was performed using the "Guideline for Post-Earthquake Damage Evaluation and Rehabilitation of RC Buildings" [6,7]. In this method, a damage class between 0 (no damage) and V (member collapse) was assigned to each member based on the observed damage, and a reduction factor, η, was assigned following the definition in Table 1. A weighted average for each floor, termed the *R* Index, was then calculated. The overall floor-level damage was then classified as slight ($R \geq 95\%$), minor ($80 \leq R < 95\%$), moderate ($60 \leq R < 80\%$), severe ($R < 60\%$), or collapsed ($R \approx 0\%$)

Table 1. Damage class and reduction factor, η [7]

Observed damage	Damage class	Reduction factor, η
None	0	1.00
< 0.2 mm	I	0.95
0.2 – 1.0 mm	II	0.75
1.0 – 2.0 mm	III	0.50
> 2.0 mm	IV	0.20
Local failure	V	0

The maximum residual crack width recorded for each member after the 1.0-scaled and 1.5-scaled events are shown in Table 2. Not all members had crack widths recorded due obstructions or health and safety issues hindering observations. Damage classes were assigned to each joint considering the largest residual crack width of the connecting beams and columns following the definitions from Table 2. This, as well as the *R* factor and the classified floor-level damage, are shown in Table 3 where "3a" and "3b" considers and ignores the hanging wall, respectively.

Based on Table 3, the damage on 1F and 2F were classified as "minor" during the 1.0-scaled excitation. On 3F, the damage was deemed "moderate" if the hanging walls were considered, and "slight" if they were ignored. In the first 1.5-scaled excitation, the damage on all floors was deemed as "moderate" or "severe". The results for the 1.6-scaled excitation were not shown as the damage was deemed "severe" based on the significant damage observed.

4.2 Capacity curve approach

A second method to assess the building damage was performed using a method proposed by Kusunoki et al. [8], where data from acceleration sensors were used to derive a representative acceleration versus displacement response curve. This is shown in Fig. 10 using different sensors (LAM02 and ADXL335), though both showed similar results.

The peak response during the 1.0-scaled event (100%) was not yet in the inelastic range, indicating slight to minor damage. After the first 1.5-scaled event (150%), the ductility response was around 2.0-3.0, indicating moderate to severe damage. Finally, significant inelastic response occurred during the 1.6-scaled event (160%), and strength decrease was observed in the positive direction, indicating severe/near collapse damage. These observations were consistent with those from visual inspections.

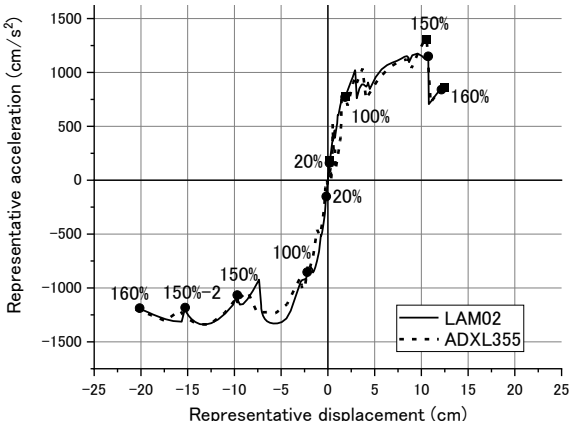

Fig. 10 Representative acceleration-displacement curve

Table 2. Largest residual crack widths for exterior structural members parallel to loading direction in mm (3 HW indicates residual crack widths in 3F hanging walls)

Event	Floor	Beam				Column					
		A1-A2	A2-A3	B1-B2	B2-B3	A1	A2	A3	B1	B2	B3
1.0	3 HW	0.08	1.00	0.85	0.80	N/A					
	3	0.08	-	-	-	-	0.06	0.04	-	-	-
	2	0.20	-	0.04	-	-	-	-	-	-	-
	1	0.50	0.55	-	-	0.20	-	0.15	-	-	0.05
1.5 run 1	3 HW	2.20	3.50	4.00	2.00	N/A					
	3	0.75	-	1.00	-	0.45	0.15	2.00	0.10	3.00	0.06
	2	2.00	3.50	2.50	-	0.15	0.04	0.15	0.15	0.10	0.15
	1	6.00	6.00	-	-	6.00	0.75	0.55	0.50	0.08	0.15

Table 3. Estimation of R factors (3a considers hanging wall while 3b is considering beam only)

Event	Floor	Joint						$\Sigma\eta_j$	$R= 100\% \times \Sigma\eta_j/N$	Classification
		A1	A2	A3	B1	B2	B3			
1.0	3a	I	III	III	II	II	II	4.2	70%	Moderate
	3b	I	I	I	I	I	I	5.7	95%	Slight
	2	II	II	I	I	I	I	5.3	88%	Minor
	1	II	II	II	I	I	I	5.1	85%	Minor
1.5 run 1	3a	IV	IV	IV	IV	IV	IV	1.2	20%	Severe
	3b	II	II	III	III	IV	I	3.7	61%	Moderate
	2	IV	IV	IV	IV	IV	I	2.0	33%	Severe
	1	IV	IV	IV	II	I	I	3.3	54%	Severe

5. DISCUSSION

Based on damage evaluations, the building's capability to achieve functionality and life-safety performance objectives can be judged. While no damage observations were performed for the 0.2-scaled excitation case, the mostly elastic response during the 1.0-scaled excitation indicated that the building should satisfy functionality performance objectives at both 0.2 and 1.0-scaled excitations. The evaluated damage was judged to be severe after the first 1.5-scaled excitation despite the building surviving two further excitations of equal or greater intensity; which would have satisfied life-safety objectives from a performance viewpoint. This was due to deformation concentrating on few cracks. To produce a better outcome, either (i) the concrete-filled slit detailing could be applied to other floors, or (ii) the slit width could be increased to allow more distributed cracking. The latter has additional benefits from reducing bar slippage which may increase hysteretic damping and reduce the building's response, though there might be insulation and weather proofing issues.

Another discussion point is whether the 3F hanging wall should be considered for damage evaluations. On one hand, there were no reinforcing bars going through the hanging-wall crack, meaning that it does not affect the member's positive flexural strength (tension at bottom). On the other, assessors may not be aware of such detailing when performing evaluations. Thus, the assessors may be more likely to use the hanging wall crack widths instead. Therefore, use of the hanging wall crack widths for damage assessments may be more reflective of field practice even though it is a less accurate representation.

Finally, it was observed that both damage evaluation methods produced similar outcomes. Given the relative ease of applying the latter (provided acceleration sensors have been installed), it gives confidence that this rapid evaluation approach is can be reliably used to assess a building's margin of safety. This will be useful in regions with dense building stock to significantly reduce the time required for post-earthquake damage evaluations.

6. CONCLUSION

Based on the findings from the shake-table tests of a building with post-disaster functions performed at E-Defense, it was found that:

(i) The presence of gaps or terminating flexural reinforcing bars at the ends of hanging and standing walls and at the base of wing-walls helped the specimen achieve objectives for buildings with post-disaster functions from a performance viewpoint;

(ii) Filling the gap with concrete decreased the compression strain demands at the soffit of beams due to allowing hanging walls to act in compression, but in turn caused more cracks to form in the hanging walls;

(iii) Structural member damage was concentrated on few cracks. This resulted in the specimen being assessed as having "severe" damage after the first 1.5-scaled excitation following damage evaluation guidelines despite being able to survive two more excitations of equal or greater intensity.

ACKNOWLEDGEMENT

The present work is supported by the Tokyo Metropolitan Resilience Project of the National Institute for Earth Science and Disaster Resilience (NIED).

REFERENCES

[1] Ministry of Land, Infrastructure, Transport and Tourison., "Design guideline for buildings with post-disaster functions (draft)", Technical Note of National Institute for Land and Infrastructure Management No. 1004, 2018

[2] Kono, S., Kitamura, F., Yuniarsyia, E., Watanabe, H., Mukai, T., and Mukai, D. J., "Efforts to Develop Resilient Reinforced Concrete Building Structures in Japan," proceedings of SMAR 2017 - Fourth Conference on Smart Monitoring, Assessment and Rehabilitation of Civil Structures, Zurich, Switzerland, 2017

[3] Tani, M., Mukai, T., Demizu, T., Kono, S., Kinugasa, H., and Maeda, M., "Full-scale Static Loading Test on a Five Story Reinforced Concrete Building (part 2: damage analysis)," proceedings of 16th World Conference on Earthquake Engineering, Santiago, Chile, 2017

[4] Hirata, N. "Introduction to the Tokyo Metropolitan Resilience Project", NHERI-NIED Plenary Session Presentation, 2017 [powerpoint presentation]

[5] Fukai, S., Kusunoki, K., and Yeow, T. Z. "A new safety evaluation system and the continuous functionality of buildings with post-disaster functions following earthquakes (part 1 – test specimen design)", proceedings of the 2019 Architectural Institute of Japan Conference, Kanazawa, Japan, 2019

[6] Maeda, M., and Kang, D.E. "Post-earthquake damage evaluation of reinforced concrete buildings", Journal of Advanced Concrete Technology, Vol 7(3), pp 327-335, 2009

[7] Maeda, M., and Matsukawa, K. "An overview of post-earthquake damage and residual capacity evaluation for reinforced concrete buildings in Japan," proceedings of 2019 Pacific Conference on Earthquake Engineering, Auckland, new Zealand, 2019.

[8] Kusunoki, K., Hinata, D., Hattori, Y., and Tasai, A. "A new method for evaluating the real-time residual seismic capacity of existing structures using accelerometers: structures with multiple degrees of freedom", Japan Architectural Review, Vol 1(1), pp 77-86, 2018